Computational accuracy and effciency for Diffraction Transfer Matrix using hybrid source-dipole formulations

Liu, Yingyi
Research Institute for Applied Mechanics, Kyushu University

Liang, Hui
Technology Centre for Offshore and Marine

Kashiwagi, Masashi
Department of Naval Architecture & Ocean Engineering, Osaka University

Cong, Peiwen
State Key Laboratory of Coastal and Offshore Engineering, Dalian University of Technology

出版情報：The 36th International Workshop on Water Waves and Floating Bodies : IWWWFB36, 2021-04-25. The International Workshop on Water Waves and Floating Bodies : IWWWFB
バージョン：
権利関係：

Computational accuracy and efficiency for Diffraction Transfer Matrix using hybrid source-dipole formulations

Yingyi Liu[a]†, Hui Liang[b], Massashi Kashiwagi[c] and Peiwen Cong[d]

[a]Research Institute for Applied Mechanics, Kyushu University, Fukuoka 8168580, Japan
[b]Technology Centre for Offshore and Marine, Singapore (*TCOMS*), 118411, Singapore
[c]Department of Naval Architecture & Ocean Engineering, Osaka University, Osaka 5650871, Japan
[d]State Key Laboratory of Coastal and Offshore Engineering, Dalian University of Technology, Dalian 116024, China

1. INTRODUCTION

The interaction theory presented by Kagemoto & Yue (1986) significantly reduces the computational burden in the wave interaction problem of multiple surface-piercing bodies, particularly arrays of wave energy converters in recent years. One of the essential operators is the so-called Diffraction Transfer Matrix (DTM). Many subsequent researchers (Goo & Yoshida 1990; Flavià *et al.* 2018) have implemented the theory using the source distribution method in evaluating the two linear operators of a single unique geometry. However, nowadays, a great majority of boundary element method codes have been written by virtue of the hybrid source-dipole distribution method (i.e., potential formulation) taking account of its high accuracy (Dai & Duan 2008).

There are basically two ways to solve the scattering potential in the potential formulation: (1) using the conventional method and then obtain the diffraction potential, or (2) solve directly the diffraction potential by applying incident-wave potential as the forcing term on the right-hand side of the boundary integral equation. The two ways are similar in wave analysis with a single body (Lee & Newman 2005) in accuracy, but the latter one runs a bit faster than the first because there is no need to evaluate the normal derivative and its integration over the wetted surface. However, when being applied to a multi-body problem, since the right-hand side of the boundary integral equation needs to be evaluated for hundreds and thousands of times, the difference of computation time can be increased substantially. In this regard, it is necessary to check how this difference could be, such that the equivalence of the two alternative approaches may need to be reappraised.

2. THEORY AND METHODOLOGY

Wave diffraction of arbitrary-geometric three-dimensional floating structures can be solved by the following hybrid source-dipole boundary integral equation in frequency domain within the framework of potential flow theory:

$$2\pi\varphi_j^S(\boldsymbol{x}) + \iint\!\!\!\!\!\!\diagup_{S_{B_j}} \varphi_j^S(\boldsymbol{\xi})\frac{\partial G(\boldsymbol{x},\boldsymbol{\xi})}{\partial n_{\boldsymbol{\xi}}}\mathrm{d}S = -\iint_{S_{B_j}} \frac{\partial \varphi_j^I(\boldsymbol{\xi})}{\partial n_{\boldsymbol{\xi}}} G(\boldsymbol{x},\boldsymbol{\xi})\mathrm{d}S \quad \text{with} \tag{1}$$

where $\boldsymbol{x} = (x, y, z)$ and $\boldsymbol{\xi} = (\xi, \eta, \zeta)$ represent the field point and the source point, respectively; $G(\boldsymbol{x}, \boldsymbol{\xi})$ is the free-surface Green function, and can be expressed in polar coordinates in terms of $\boldsymbol{x} = (x, y, z) = (r\cos\theta, r\sin\theta, z)$ and $\boldsymbol{\xi} = (\xi, \eta, \zeta) = (R\cos\Theta, R\sin\Theta, \zeta)$ following Fenton (1978), in the form of

$$\begin{aligned} G =& 2\pi\mathrm{i}C_0\cosh k(z+h)\cosh k(\zeta+h)\sum_{m=-\infty}^{\infty}\begin{Bmatrix} J_m(kR)H_m^{(1)}(kr) \\ H_m^{(1)}(kR)J_m(kr)\end{Bmatrix}\mathrm{e}^{\mathrm{i}m(\theta-\Theta)} \\ &+ 4\sum_{n=1}^{\infty} C_n\cos k_n(z+h)\cos k_n(\zeta+h)\sum_{m=-\infty}^{\infty}\begin{Bmatrix} J_m(k_nR)K_m(k_nr) \\ K_m(k_nR)J_m(k_nr)\end{Bmatrix}\mathrm{e}^{\mathrm{i}m(\theta-\Theta)}. \end{aligned} \tag{2}$$

The upper terms in the curly braces are used when $r \geqslant R$ (the region outside of a circular cylinder that circumscribes the body or bodies) and the lower terms when $r < R$.

2.1. *Partial waves in cylindrical harmonics*

In a finite-sized array of floating bodies, it is convenient to express the velocity potentials as the scalar product between a vector of complex coefficients and a vector of partial cylindrical wave component (Flavià *et al.* 2018):

$$\phi_j^I = \{A_j^I\}^T\{\varphi_j^I\}, \quad \phi_j^S = \{A_j^S\}^T\{\varphi_j^S\}, \tag{3}$$

where the superscript T represents the matrix transpose operator, the curly brace $\{\cdot\}$ stands for a vector and the subscript j denotes the jth body. $\{A_j^I\}$ and $\{A_j^S\}$ are the complex incident and scattered vectors of partial wave coefficients. Indexes (l, q) are associated with incident waves and (n, m) with outgoing waves. The vectors of the incident and scattered cylindrical functions are respectively expressed as

$$\{\varphi_j^I\}_{lq} = \begin{cases} \dfrac{\cosh k(z_j+h)}{\cosh kh}J_q(kr_j)\mathrm{e}^{\mathrm{i}q\theta_j} & l = 0, \\ \cos k_l(z_j+h)I_q(k_lr_j)\mathrm{e}^{\mathrm{i}q\theta_j} & l \geqslant 1, \end{cases} \tag{4}$$

† Email address for correspondence: liuyingyi@riam.kyushu-u.ac.jp

$$\{\varphi_j^S\}_{nm} = \begin{cases} \dfrac{\cosh k(z_j+h)}{\cosh kh} H_m^{(1)}(kr_j)\mathrm{e}^{\mathrm{i}m\theta_j} & n=0, \\ \cos k_n(z_j+h)K_m(k_n r_j)\mathrm{e}^{\mathrm{i}m\theta_j} & n \geqslant 1. \end{cases} \tag{5}$$

2.2. *Method I*

Derivation of the DTM of a specific floating body can be started from considering the wave diffraction by a single body. The scattering potential of a single floating body in a partial incident wave of mode (l,q) without the presence of other bodies can be expressed as

$$\begin{aligned}[\varphi_j^S(r_j,\theta_j,z_j)]_{lq} =& \frac{\cosh k(z_j+h)}{\cosh kh} \sum_{m=-\infty}^{\infty} D_{0m}^{j,lq} H_m^{(1)}(kr_j)\mathrm{e}^{\mathrm{i}m\theta_j} \\ &+ \sum_{n=1}^{\infty} \cos k_n(z_j+h) \sum_{m=-\infty}^{\infty} D_{nm}^{j,lq} K_m(k_n r_j)\mathrm{e}^{\mathrm{i}m\theta_j},\end{aligned} \tag{6}$$

where $D_{0m}^{j,lq}$ and $D_{nm}^{j,lq}$ are scattered complex coefficients. On the other hand, the scattering potential at a field point in the fluid domain (other than the body surface) can be determined by the following equation

$$\begin{aligned}[\varphi_j^S(r_j,\theta_j,z_j)]_{lq} = -\frac{1}{4\pi}\Bigg\{ &\iint_{S_B^j} [\varphi_j^S(R_j,\Theta_j,\zeta_j)]_{lq} \frac{\partial G(r_j,\theta_j,z_j;R_j,\Theta_j,\zeta_j)}{\partial n_{\boldsymbol{\xi}}} \mathrm{d}S \\ &+ \iint_{S_B^j} G(r_j,\theta_j,z_j;R_j,\Theta_j,\zeta_j) \frac{\partial [\varphi_j^I(R_j,\Theta_j,\zeta_j)]_{lq}}{\partial n_{\boldsymbol{\xi}}} \mathrm{d}S \Bigg\}\end{aligned} \tag{7}$$

Substituting Eq. (2) into Eq. (7) and comparing Eq. (6) with Eq. (7) yields

$$D_{0m}^{j,lq} = -\frac{\mathrm{i}}{2} C_0 \cosh kh \iint_{S_B^j} \left[(\varphi_j^S)_{lq} \frac{\partial}{\partial n} + \frac{\partial (\varphi_j^I)_{lq}}{\partial n} \right] [J_m(kR_j)\cosh k(\zeta_j+h)\mathrm{e}^{-\mathrm{i}m\Theta_j}] \mathrm{d}S, \tag{8}$$

$$D_{nm}^{j,lq} = -\frac{1}{\pi} C_n \iint_{S_B^j} \left[(\varphi_j^S)_{lq} \frac{\partial}{\partial n} + \frac{\partial (\varphi_j^I)_{lq}}{\partial n} \right] [I_m(k_n R_j)\cos k_n(\zeta_j+h)\mathrm{e}^{-\mathrm{i}m\Theta_j}] \mathrm{d}S, \tag{9}$$

where $D_{0m}^{j,lq}$ and $D_{nm}^{j,lq}$ are exactly the elements of DTM. The only unknown in Eqs. (8) and (9) is $(\varphi_j^S)_{lq}$, which can be solved by the following boundary integral equation

$$\begin{aligned}2\pi[\varphi_j^S(r_j,\theta_j,z_j)]_{lq} &+ \iint_{S_B^j} [\varphi_j^S(R_j,\Theta_j,\zeta_j)]_{lq} \frac{\partial G(r_j,\theta_j,z_j;R_j,\Theta_j,\zeta_j)}{\partial n_{\boldsymbol{\xi}}} \mathrm{d}S \\ &= -\iint_{S_B^j} \frac{\partial [\varphi_j^I(R_j,\Theta_j,\zeta_j)]_{lq}}{\partial n_{\boldsymbol{\xi}}} G(r_j,\theta_j,z_j;R_j,\Theta_j,\zeta_j) \mathrm{d}S.\end{aligned} \tag{10}$$

2.3. *Method II*

A second way of evaluating the DTM elements is to consider the following boundary integral equation, which was first proposed by (Kashiwagi & Kohjo 1995):

$$C(r_j,\theta_j,z_j)[\varphi_j^D(r_j,\theta_j,z_j)]_{lq} + \iint_{S_B^j} [\varphi_j^D(R_j,\Theta_j,\zeta_j)]_{lq} \frac{\partial G(r_j,\theta_j,z_j;R_j,\Theta_j,\zeta_j)}{\partial n_{\boldsymbol{\xi}}} \mathrm{d}S = 4\pi[\varphi_j^I(r_j,\theta_j,z_j)]_{lq}, \tag{11}$$

where $(\varphi_j^D)_{lq}$ is the total diffraction potential in correspondence to the partial incident wave of mode (l,q). Following a similar process, the DTM elements can be derived as

$$D_{0m}^{j,lq} = -\frac{\mathrm{i}}{2} C_0 \cosh kh \iint_{S_B^j} [(\varphi_j^S)_{lq} + (\varphi_j^I)_{lq}] \frac{\partial}{\partial n} [J_m(kR_j)\cosh k(\zeta_j+h)\mathrm{e}^{-\mathrm{i}m\Theta_j}] \mathrm{d}S, \tag{12}$$

$$D_{nm}^{j,lq} = -\frac{1}{\pi} C_n \iint_{S_B^j} [(\varphi_j^S)_{lq} + (\varphi_j^I)_{lq}] \frac{\partial}{\partial n} [I_m(k_n R_j)\cos k_n(\zeta_j+h)\mathrm{e}^{-\mathrm{i}m\Theta_j}] \mathrm{d}S, \tag{13}$$

3. RESULTS AND DISCUSSIONS

In order to verify the present method based on the hybrid source-dipole boundary integral equation (Liu 2019; Liang *et al.* 2020), numerical computations are performed against two benchmark problems given in Flavià *et al.* (2018). In Figs. 1, 'Present' stands for the numerical results generated using 'Method I', as the megascopic difference between the results of 'Method I' and 'Method II' are indistinguishable.

The real and imaginary parts of the DTM terms of the truncated vertical cylinder are shown in Figs. 1. In general, a good agreement is found between results computed by the methods of McNatt *et al.* (2015) and Flavià *et al.* (2018), respectively. Exceptions occur with Flavià *et al.* (2018) at some specific frequencies, e.g., $ka = 2.39, 2.57, 2.75$. This should be attributed to the 'irregular frequencies' phenomenon, as Flavià *et al.* (2018) was using the open-source BEM code Nemoh (Babarit & Delhommeau 2015), which at that time did not have

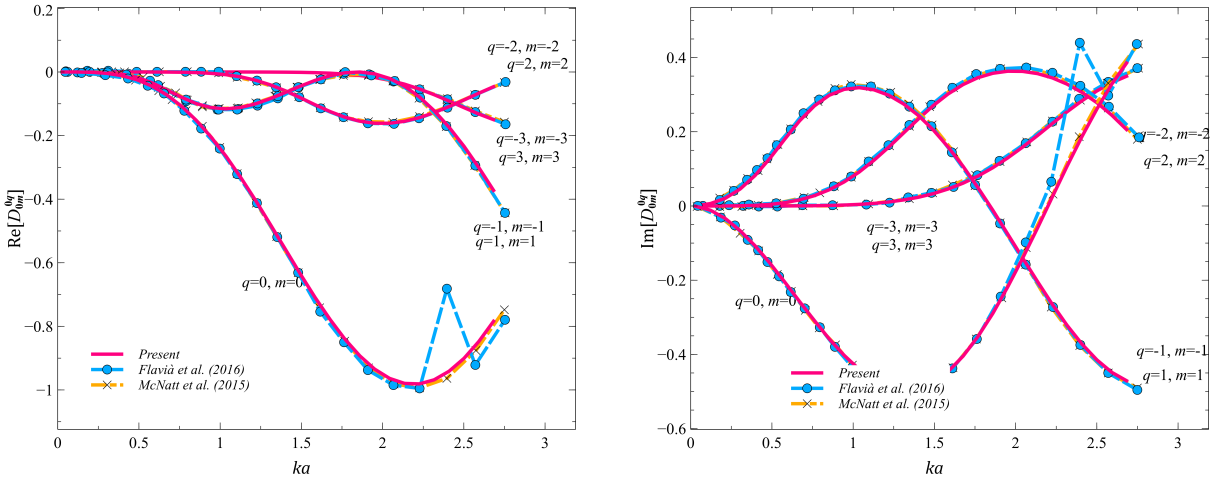

Figure 1: DTM progressive terms for a truncated vertical cylinder of 3 m radius, 6 m draft in a 10 m water depth: (a) real part; (b) imaginary part.

	Re $q=0$, $m=0$			Im $q=0$, $m=0$		
ka	Method I	Method II	Error	Method I	Method II	Error
0.6	−0.049621	−0.04971	−0.18%	−0.21695	−0.21741	−0.21%
1.2	−0.3895	−0.39203	−0.65%	−0.48501	−0.48828	−0.67%
1.8	−0.85964	−0.87157	−1.39%	−0.33147	−0.33618	−1.42%
2.4	−0.94447	−0.96528	−2.20%	0.17974	0.18373	−2.22%
3.0	−0.50805	−0.52609	−3.55%	0.4822	0.49947	−3.58%

Table 1: Comparison of the first two diagonal terms of the DTM between Method I and Method II, with an incident wave heading angle 0 degree.

the 'irregular frequencies removal' functionality (Penalba *et al.* 2017). Nevertheless, the agreement between the present results and those of McNatt *et al.* (2015) is pretty good with respect to all the frequencies, as the latter was using WAMIT® with the 'irregular frequencies' being removed.

The difference of numerical results between the two methods in computation of the DTM of the truncated vertical cylinder is assesed in Table 1. Only the first two diagonal terms with $q=0$, $m=0$ and $q=1$, $m=1$ (i.e., D_{00}^{00} and D_{01}^{01}) are compared since they are the largest terms of the DTM. In general, the absolute value of Method I's result is less than that of Method II. The absolute relative error increases against the wave number ka but is still acceptable around $ka=3.0$ ($\omega=3.132$ rad/s). As it is known that the upper limit (at which the spectrum approaches zero) of a typical wave spectrum can normally be below $\omega=2.5$ rad/s, an absolute relative error of the DTM term below 5.0% means that using either of the methods can be fine for the calculation.

Fig. 2 shows the CPU time of per evaluation of the DTM of the floating square box at different stages, on a desktop machine, with the aid of OpenMP parallelism on eight threads. In Fig. 2, Eq. (6) is truncated with a maximum depth mode of $N_{\text{Max}}=5$ and a maximum angular mode of $M_{\text{Max}}=5$, indicating that the number of diffraction problems to be solved at each frequency is $(N_{\text{Max}}+1)(2M_{\text{Max}}+1)N_{\text{WaveHeadings}}=2376$ and the number of the diffraction transfer matrices to be calculated is $N_{\text{WaveHeadings}}=36$. Assembling the right-hand side matrix takes up most of the time (93.90% of the overall computation time) in Method I, while solving the linear algebraic system costs the most in Method II. In Table 2, the total CPU time and the percentage of 'assembling the right-hand side matrix' increase rapidly in Method I with respect to the truncation mode. While the total CPU time of Method I is twice that of Method II when $N_{\text{Max}}=0$, it increases significantly to 15.75 times that of Method II when $N_{\text{Max}}=10$. For Method I, the percentage of 'assembling the right-hand side matrix' quickly increases to above 90% as the truncation mode increases merely to 3. Method I is much more computationally expensive due to the more complex right-hand side of the boundary integral equation.

4. CONCLUSIONS

Evaluating the DTM using hybrid source-dipole formulations is presented and good agreement is found between the source-distribution method. Two alternative ways of computing the DTM are compared, showing that while the accuracy does not differ much, the computation cost can be substantially saved by using the approach proposed in Kashiwagi & Kohjo (1995). Moreover, it is found that when more terms of DTM are needed, the increase of the truncation mode can lead to a significant increase of the overall CPU time, for which issue applying the conventional approach may not be acceptable anymore.

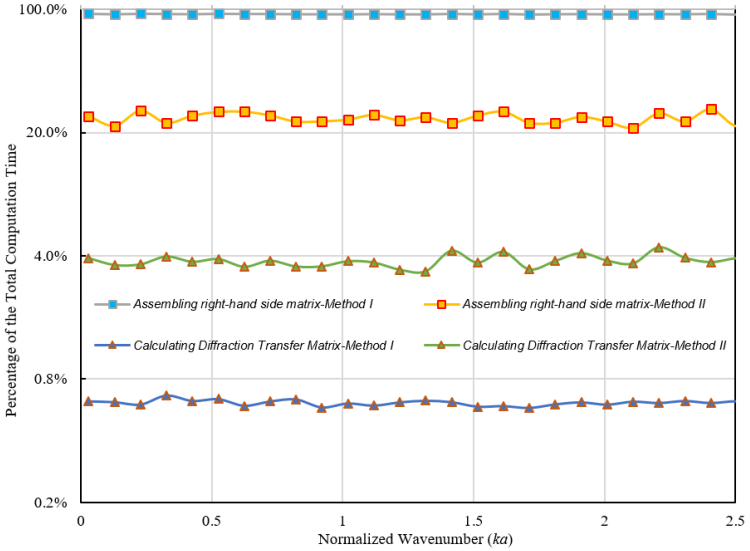

Figure 2: Percentages of the time cost in the per-frequency diffraction computation using the two methods.

N_{Max}, M_{Max}	CPU Time Method I	CPU Time Method II	Assembling right-hand side matrix Method I	Assembling right-hand side matrix Method II	Calculating DTM Method I	Calculating DTM Method II
0	23.12 (s)	12.31 (s)	39.53%	1.39%	15.29%	13.75%
1	70.75 (s)	15.10 (s)	77.50%	6.78%	5.00%	11.21%
2	156.48 (s)	20.12 (s)	87.60%	12.71%	2.26%	8.41%
3	280.32 (s)	27.37 (s)	91.28%	17.44%	1.26%	6.18%
4	442.26 (s)	36.85 (s)	92.99%	20.82%	0.80%	4.59%
5	642.31 (s)	48.57 (s)	93.90%	23.17%	0.55%	3.48%
10	2214.10 (s)	140.60 (s)	95.35%	28.01%	0.16%	1.20%

Table 2: Increase of the time cost of per-frequency (e.g., $ka = 0.921$) DTM computation against the maximum truncation mode: the 2nd and 3rd columns give the total CPU times using Method I and II; the rest 4th–7th columns give the percentage of the time cost in the total CPU times at different stages using the two methods.

ACKNOWLEDGEMENTS

This work was supported by Grant-in-Aid for Early-Career Scientists (JSPS Grant Number JP18K13939).

REFERENCES

Babarit, A. & Delhommeau, G. 2015 Theoretical and numerical aspects of the open source BEM solver NEMOH. In *Proceeding of the 11th European Wave and Tidal Energy Conference, Nantes, France*.

Dai, Y. S. & Duan, W. Y. 2008 *Potential flow theory of ship motions in waves*. National Defense Industry Publication.

Fenton, J. D. 1978 Wave forces on vertical bodies of revolution. *Journal of Fluid Mechanics* **85** (2), 241–255.

Flavià, F. F., McNatt, C., Rongère, F., Babarit, A. & Clément, Al. H. 2018 A numerical tool for the frequency domain simulation of large arrays of identical floating bodies in waves. *Ocean Engineering* **148**, 299–311.

Goo, J.-S. & Yoshida, K. 1990 A numerical method for huge semisubmersible responses in waves. *Transactions-Society of Naval Architects and Marine Engineers* **98**, 365–387.

Kagemoto, H. & Yue, D. K. P. 1986 Interactions among multiple three-dimensional bodies in water waves: an exact algebraic method. *Journal of Fluid Mechanics* **166**, 189–209.

Kashiwagi, M. & Kohjo, T. 1995 A calculation method for hydrodynamic interactions of multiple bodies supporting a huge floating body (in japanese) pp. 247–254.

Lee, C. H. & Newman, J. N. 2005 Computation of wave effects using the panel method. *Numerical Models in Fluid Structure Interaction* **42**, 211–251.

Liang, H., Ouled Housseine, C., Chen, X. B. & Shao, Y. 2020 Efficient methods free of irregular frequencies in wave and solid/porous structure interactions. *Journal of Fluids and Structures* **98**, 103130.

Liu, Y. 2019 HAMS: a frequency-domain preprocessor for wave-structure interactions – theory, development, and application. *Journal of Marine Science and Engineering* **7** (3), 81.

McNatt, J. C., Venugopal, V. & Forehand, D. 2015 A novel method for deriving the diffraction transfer matrix and its application to multi-body interactions in water waves. *Ocean Engineering* **94**, 173–185.

Penalba, M., Kelly, T. & Ringwood, J. 2017 Using NEMOH for modelling wave energy converters: A comparative study with WAMIT. In *Proceeding of the 12th European Wave and Tidal Energy Conference (EWTEC2017), Cork, Ireland*.